Polar Solute Transport Across the Pigmented Rabbit Conjunctiva: Size Dependence and the Influence of 8-Bromo Cyclic Adenosine Monophosphate

Yoshihide Horibe,[1] Ken-ichi Hosoya,[1,8] Kwang-Jin Kim,[2,4,5,6] Taro Ogiso,[7] and Vincent H. L. Lee[1,3,9]

Received April 19, 1997; accepted June 14, 1997

Purpose. To characterize the conjunctival permeability to polar solutes ranging from 182 to 167,000 daltons in molecular weight (m.w.).
Methods. Solute transport across the excised pigmented rabbit conjunctiva with a baseline transepithelial electrical resistance (TEER) of 1,285 ± 46 ohm·cm^2 was evaluated in the modified Ussing chamber under open-circuit conditions. The model solutes were mannitol (m.w. 182), 6-carboxyfluorescein (m.w. 376), and fluorescein isothiocyanate-labeled dextrans (FD4, m.w. 4,400—FD150, m.w. 167,000).
Results. For a given solute, the apparent permeability coefficient (Papp) was independent of solute concentration and direction of transport. As expected, the Papp decreased with solute size, from 27.7 × 10^{-8} cm/sec for mannitol to 0.31 × 10^{-8} cm/sec for FD150. When the experimental temperature was lowered from 37°C to 4°C, Papp decreased by ~50% for FD4 through FD40 and by >80% for both FD70 and FD150. Equivalent pore analysis, assuming restricted solute diffusion via cylindrical, water-filled pores across the isolated tissue, revealed a radius of 5.5 nm at a pore density of 1.9 × 10^8 pores per cm^2. The addition of 1 mM 8-bromo cyclic adenosine monophosphate (8-BrcAMP), known to stimulate Cl^- secretion and decrease TEER, to the mucosal side of the conjunctiva increased the transport of mannitol, FD4, and FD40 by 28%, while not affecting FD150 transport.
Conclusions. Our findings suggest that polar solutes up to FD40 traverse the conjunctival epithelial barrier primarily by restricted diffusion through equivalent pores of 5.5 nm radius and that solute movement is affected by reduction of TEER. On the other hand, polar solutes of the FD70 or larger may cross the barrier primarily via non-diffusional pathways such as non-specific endocytosis.

[1] Department of Pharmaceutical Sciences, School of Pharmacy, University of Southern California, Los Angeles, California 90033.
[2] Will Rogers Institute Pulmonary Research Center, University of Southern California, Los Angeles, California 90033.
[3] Department of Ophthalmology, University of Southern California, Los Angeles, California 90033.
[4] Department of Medicine, School of Medicine, University of Southern California, Los Angeles, California 90033.
[5] Department of Physiology and Biophysics, University of Southern California, Los Angeles, California 90033.
[6] Department of Biomedical Engineering, School of Engineering, University of Southern California, Los Angeles, California 90033.
[7] Faculty of Pharmaceutical Sciences, Kinki University 3-4-1 Kowakae, Higashi-Osaka 577, Japan.
[8] Present Address: Department of Pharmaceutics, Faculty of Pharmaceutical Sciences, Tohoku University, Aoba, Aramakiaza, Aoba-ku, Sendai 980-77 Japan.
[9] To whom correspondence should be addressed. (e-mail: vincentl@hsc.usc.edu)

KEY WORDS: conjunctival epithelium; conjunctival drug delivery; cyclic adenosine monophosphate; equivalent pores.

INTRODUCTION

Topically applied drugs can reach the intraocular tissues by either the corneal and/or the noncorneal (conjunctival-scleral) pathways. The ratio of drug amount in the iris-ciliary body absorbed through the corneal and noncorneal pathways was 70:1 for hydrocortisone (1), 12:1 for timolol (2), and 5:1 for pilocarpine (1). By contrast, inulin was absorbed by only the noncorneal pathway (2,3). The bulbar conjunctiva is the first tissue across which a topically applied drug must pass in order to reach the underlying tissues in the uveal tract (4). Previous work in our laboratory revealed that the conjunctiva was permeable to a variety of molecules (beta blockers, peptides, and proteins) differing in size and polarity (5,6). Although the conjunctival permeability to polar solutes was previously investigated, those studies were conducted either over a restricted size range of the solutes (less than 1,000 daltons) (7) or under conditions that might have compromised tissue integrity (3,7,8). In fact, the estimated pore size in the rabbit conjunctiva reported by Hämäläinen *et al.* (7) was outside of the size range spanned by the model solutes they utilized. The conclusions drawn from such studies on the feasibility of delivering proteins and oligonucleotides via the paracellular pathway in the conjunctiva to the posterior segment of the eye may, therefore, be incorrect.

Thus, the purpose of the present study was to characterize the transport of polar solutes, ranging from 182 to 167,000 daltons in molecular weight, across the excised pigmented rabbit conjunctiva (whose baseline transepithelial electrical resistance (TEER) was 1,285 ± 46 ohm·cm^2) under conditions that assured tissue viability and integrity. The model solutes were mannitol (m.w. 182), 6-carboxyfluorescein (m.w. 376), and fluorescein isothiocyanate-labeled dextrans (FDs) ranging from 4,400 to 167,000 daltons in molecular weight. In addition, the effect of 8-bromo cyclic adenosine monophosphate (8-BrcAMP), known to stimulate Cl^- secretion in the conjunctival epithelium while reducing the TEER (9), on transconjunctival polar solute transport was also evaluated. Several studies have shown that an increase in cell cAMP leads to a decrease in TEER (10–12) or to an increase in paracellular permeability for a variety of cell types (13,14). Varlet *et al.* (15) showed that dibutyryl cAMP significantly decreased TEER, thereby causing a concomitant increase in apical-to-basal inulin flux in corneal endothelial cells.

MATERIALS AND METHODS

Animals

Male pigmented rabbits, weighing 2.5–3.0 kg, were purchased from Irish Farms (Los Angeles, CA). The investigations utilizing rabbits described in this report conformed to the Guiding Principles in the Care and Use of Animals (DHEW Publication, NIH 80–23).

Chemicals

6-Carboxyfluorescein (6-CF), fluorescein isothiocyanate(FITC)-labeled dextrans (FD) with average molecular

0724-8741/97/0900-1246$12.50/0

weights of 4,400 (FD4), 9,400 (FD10), 21,200 (FD20), 38,620 (FD40), 71,200 (FD70), and 167,000 (FD150), and 8-bromo cyclic adenosine monophosphate (8-BrcAMP) were purchased from Sigma Chemical Co. (St. Louis, MO). The FITC content was in the range of 0.004–0.013 mole per mole of glucose. D-[1-^{14}C]-Mannitol (56 mCi/mmol) was purchased from Moravek Biochemicals (Brea, CA).

Solutions

Unless otherwise indicated, all experiments were conducted with bicarbonated Ringer's solution maintained at 37°C and pH 7.4 under 95% air/5% CO_2. The bicarbonated Ringer's solution contained 111.5 mM NaCl, 4.8 mM KCl, 0.75 mM NaH_2PO_4, 29.2 mM $NaHCO_3$, 1.04 mM $CaCl_2$, 0.74 mM $MgCl_2$, and 5 mM D-glucose. The osmolality of solution was about 300 mOsm/kg H_2O.

Tissue Preparation

We have previously reported detailed procedures for isolating and preparing the rabbit conjunctiva for mounting in the modified Ussing chamber (16), a process which usually was completed within 15 min. Briefly, rabbits were killed with an injection of 85 mg/kg of sodium pentobarbital into a marginal ear vein. The entire eye ball was removed from the orbit taking care not to damage the conjunctival epithelium. The excised conjunctiva was trimmed and mounted in the tissue adapter with a circular aperture of 1.0 cm^2. The adapter-tissue assembly was then placed in a modified Ussing chamber. The bathing solution was bubbled with 5% CO_2 in air to maintain the pH at 7.4 and to provide adequate agitation of the solution. The Ussing chamber assembly was maintained at 36 ± 1°C by a water jacket using a circulating water bath.

Measurement of Bioelectric Properties of the Conjunctiva

The transport experiments were conducted under open-circuit conditions. To assess tissue viability and integrity, the spontaneously generated transepithelial electrical potential difference (PD) and resistance (TEER) were monitored with an automatic voltage clamp device (558C-5, University of Iowa, Bioengineering Department, Iowa city, IA) every 30 min during the transport experiments as well as before and at the end of each experiment. PD was taken as an index of net active ion transport and TEER as an index of the integrity of tight junctions of the isolated conjunctiva. PD was measured with two matched calomel electrodes. Two polyethylene (PE 90) bridges (containing 4% agar in 3M KCl), whose tips were located near the center of tissue surfaces, were used to electrically connect the reservoir fluid to electrode wells. The electrical output of calomel electrodes was amplified by the voltage clamp unit. Direct current was passed across the conjunctiva using a pair of matched Ag/AgCl electrodes with conducting agar bridges, whose tips were positioned away from tissue surfaces at the far ends of two reservoirs. A 2 mV pulse (ΔV) was imposed for 3 sec across the tissue to estimate TEER as a surface area normalized ratio of applied voltage pulse to the observed deflection in resultant current (ΔI) [TEER = $(\Delta V/\Delta I)A$, where A is the nominal surface area (1 cm^2) of the Ussing chamber opening]. In this study, 1.56 ± 0.06 μA of ΔI was observed in response to 2 mV of ΔV. Prior to each experiment, the solution resistance (<100 ohm·cm^2) was compensated for utilizing the automatic voltage clamp unit.

Measurement of Mannitol Fluxes

Mannitol fluxes were measured by assaying the radioactivity in 0.5 ml of the receiver fluid collected at 0.5, 1, 1.5, 2, and 3 hr following the addition of ^{14}C-mannitol (1 μCi/ml) and 10 μM unlabeled mannitol to the donor bathing fluid. Immediately after each sampling, the volume removed was replaced with an equal volume of an appropriate fresh buffer.

Measurement of 6-CF and FD Fluxes

Essentially the same procedure described for mannitol was used to measure 6-CF and FDs fluxes except that 1 ml samples were collected at each sampling time and that three additional time points—2.5, 3.5, and 4 hr—were included. The solute concentration in the donor fluid was 0.25 mg/ml for 6-CF and 1 or 5 mg/ml for the FDs. A higher concentration was chosen for the FDs for the sake of meeting the detection sensitivity (1 ng/ml). The fluorescence of the samples was measured in a fluorescence spectrophotometer (Perkin Elmer 650-10S, Norwalk, CT) at an excitation wavelength of 490 nm and an emission wavelength of 515 nm.

Determination of Intact FD Fraction in Bathing Fluids

Gel permeation chromatography (GPC) was performed on donor and receiver fluids which were pooled separately at the end of the FD flux experiments. The pooled donor fluid samples were injected into the GPC system as is, while the pooled receiver fluids were first concentrated about eight-fold by directing a gentle stream of nitrogen gas onto the surface of the solution. An aliquot (100 μl) of samples was injected into a GPC system consisted of a dual pump, a controller, and a variable wavelength UV detector (Waters, Milford, MA). A Protein-Pak 300WS column (Waters, Milford, MA) was used. The mobile phase was phosphate-buffered saline (PBS) diluted 10 times with MilliQ water. The flow rate was 0.4 ml/min. Four hundred microliter fractions of the eluant were assayed for fluorescence as described above.

Data Analysis

Unidirectional fluxes (J) for polar solutes were estimated from the steady-state slope of the cumulative amount appearing in the receiver fluid over time. The apparent permeability coefficient (Papp) was calculated by normalizing the flux against the nominal surface area (1.0 cm^2) and initial solute concentration. The activation energy (E_a) of transport was estimated from the Papp at 4°C and at 37°C according to Equation 1:

$$P_{37}/P_4 = \exp\{-E_a/R[1/(273 + 37) - 1/(273 + 4)]\} \quad (1)$$

where P is the experimental Papp (subscripts 37 and 4 denote experimental temperatures in degrees Celsius) and R is the universal gas constant.

In applying the equivalent pore radius analysis, restricted diffusion of polar solutes via cylindrical water-filled pores was assumed (17). Thus, the permeability-to-diffusion coefficient ratio at 37°C (Papp/D_{37}) of a test solute with a Stokes-Einstein

radius (r_e) for a single homogeneous population of equivalent pores (with a radius of r_p) is as follows:

$$\text{Papp}/D_{37} = (A_p/dx)(1 - u)^2(1 - 2.104u + 2.809u^3 \quad (2)$$
$$+ 0.9481u^5 - 1.372u^6)$$

where A_p is the total pore area, dx is the mean thickness of the barrier, and $u = r_e/r_p$. From the experimental Papp's and the calculated Stokes-Einstein radii of the molecules (18), the equivalent pore radius (r_p) and the ratio (A_p/dx) between total pore area and pore length were estimated on the basis of a nonlinear curve fitting procedure MULTI (19). Assuming a dx of 30 μm for the conjunctival epithelial barrier (20), the available total pore area (A_p) was calculated from the estimate of A_p/dx. Finally, the number (N_p) of equivalent pores was calculated from the relationship $N_p = A_p/(\pi r_p^2)$.

Unpaired or paired, two-tailed Student's *t*-test was used to determine the significance of differences between two data group means. $P < 0.05$ was considered as significant.

RESULTS

Conjunctival Bioelectric Properties

The baseline PD of 15.9 ± 0.6 mV (mucosal side negative) and TEER of 1,285 ± 46 ohm·cm^2 were observed for 73 conjunctival tissues used in this study, which were comparable to those obtained for our previous studies (16,21). The presence of polar solutes in either the mucosal or serosal donor fluid elicited no significant effects on bioelectric properties. At 4°C, PD decreased to zero and TEER increased by about 50%, suggesting inhibition of active ion absorption without significant derangement of functional tight junctions. The observed 50% increase in TEER was likely due to decreased ionic diffusion or increased sealing capacity of tight junctional complex at low temperature (22).

Effect of Molecular Size on Polar Solute Transport

The transport profiles of FD in the mucosal-to-serosal (ms) and serosal-to-mucosal (sm) directions showed typical pseudo steady-state characteristics with a lag time of about 60–90 min (Fig. 1). The cumulative FD appearing in the receiver fluid became commensurately smaller as the size of dextrans was increased. The transport profiles of mannitol and 6-CF in the ms and sm directions showed a similar pattern to that of FD (data not shown). There was no significant difference between the Papp in the ms and the sm directions for each of the solutes studied (Table 1). The Papp decreased gradually from 27.7×10^{-8} cm/s for mannitol to 0.40×10^{-8} cm/s for FD40. The Papp was 0.30×10^{-8} cm/s for both FD70 and FD150. Moreover, the ms Papp for FD4 and FD40 was not siginificantly different between 1 and 5 mg/ml of donor concentrations ($p > 0.05$).

Assessment of FD Degradation

The fluorescence chromatograms of the mucosal donor and serosal receiver fluids collected at the end of the mucosal-to-serosal transport experiment are shown in Fig. 2. Based on the area under the curve, >90% of the fluorescence in the serosal receiver fluid and 100% of the fluorescence in the mucosal donor fluid, respectively, were associated with intact FD. In the serosal-to-mucosal transport experiment, the mucosal receiver fluid contained >90% intact FD and the serosal donor fluid exhibited no degradation (data not shown).

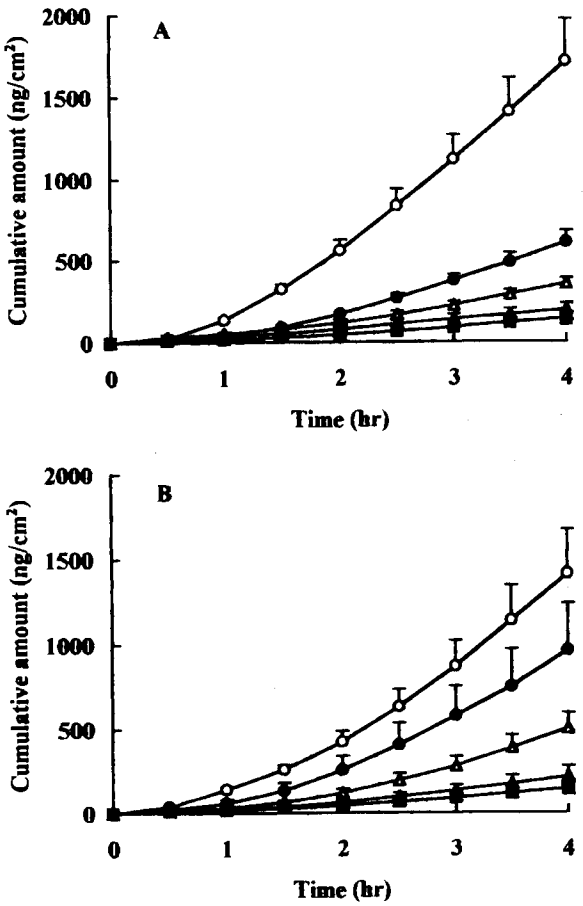

Fig. 1. Time courses of accumulation of FITC-labeled dextrans (FD) in serosal (A) or mucosal (B) receiver fluid at 5 mg/ml FD in the donor fluid. Each data point represents mean ± s.e.m (n = 3–5). (○: FD4, ●: FD10, △: FD20, ▲: FD40, □: FD70, ■: FD150).

Effect of Temperature on FD Transport

When the experimental temperature was lowered to 4°C, the Papp for dextrans decreased in a size-dependent manner (Fig. 3), being >80% for both FD70 and FD150 and ~50% for FD4 through FD40. The activation energy of transport was 9 kcal/mol for both FD70 and FD150 and was 3 kcal/mole for FD4 through FD40.

Equivalent Pore Radius

The relationship between log Papp and the solute radii is depicted in Fig. 4. The curve shows the theoretical relationship predicted by simple restricted diffusion of mannitol to FD40 through water-filled, cylindrical pores with a radius of 5.5 ± 0.3 nm. FD70 and FD150 were excluded from the equivalent pore analysis, since the greater temperature effect on Papp for these two solutes suggests translocation via predominantly non-diffusional pathway. The estimated ratio of total pore area over pore length, Ap/dx, was 0.06 cm. Based on a mean thickness

Table 1. Apparent Permeability Coefficients for Polar Solutes to the Pigmented Rabbit Conjunctiva and Effects of Mucosally-Added 1 mM 8-BrcAMP on the Transepithelial Electrical Resistance and Solute Transport in the Mucosal-to-Serosal Direction

Solutes	Molecular weight (daltons)	Radius (nm)	Donor concentration (mg/ml)	Papp ($\times 10^{-8}$ cm/s)[a]		Percent change from baseline when 1 mM 8-BrcAMP was added to mucosal side	
				ms[b]	sm[c]	Papp	TEER[d]
Mannitol	182	0.43	0.005	27.70 ± 4.33	25.50 ± 4.40	23 ± 9 ↑	20 ± 5 ↓
6-CF	376	0.68	0.25	15.70 ± 3.30	12.46 ± 2.35	—[e]	—[e]
FD4	4,400	1.44	1	3.41 ± 0.79	—[e]	—[e]	—[e]
			5	3.51 ± 0.62	3.09 ± 0.65	31 ± 2 ↑	29 ± 1 ↓
FD10	9,400	1.91	5	1.91 ± 0.26	2.08 ± 0.51	—[e]	—[e]
FD20	21,200	2.44	5	0.71 ± 0.06	0.89 ± 0.11	—[e]	—[e]
FD40	38,260	2.95	1	0.42 ± 0.08	—[e]	—[e]	—[e]
			5	0.40 ± 0.06	0.44 ± 0.13	29 ± 6 ↑	28 ± 3 ↓
FD70	71,200	3.81	5	0.30 ± 0.02	0.28 ± 0.08	—[e]	—[e]
FD150	167,000	4.94	5	0.31 ± 0.01	0.28 ± 0.07	3 ± 2 ↑	21 ± 3 ↓

Note: ↑ Relative increase from the corresponding baseline value. ↓ Relative decrease from the corresponding baseline value.
[a] Apparent permeability coefficient. Results represent mean ± s.e.m. (n = 3–5).
[b] Parameters measured in the mucosal-to-serosal direction.
[c] Parameters measured in the serosal-to-mucosal direction.
[d] Transepithelial electrical resistance.
[e] Not determined.

of 30 μm for the barrier (20), the number (N_p) of equivalent pores was $1.9 \times 10^8/cm^2$.

Effect of 8-BrcAMP on Polar Solute Transport

As shown in Table 1, the addition of 1 mM 8-BrcAMP to the mucosal side of the pigmented rabbit conjunctiva significantly decreased TEER by 20–29% and concurrently increased the ms transport of mannitol, FD4, and FD40 by 23–31% ($p < 0.01$), while not affecting the ms transport of FD150 ($p > 0.05$).

DISCUSSION

We have investigated the influence of molecular size on the conjunctival transport of polar solutes under conditions that assure the viability and integrity of the tissue during the flux experiments. On the basis of lack of concentration and directionality dependence of transport (Table 1), FD's in the size range of FD4 and FD40 probably traverse the pigmented rabbit conjunctiva by restricted passive diffusion. The gradual decrease in the log Papp against the increase in solute radius for up to FD40, as shown in Fig. 4, suggests an inverse relation between Papp vs. molecular size. Moreover, given their hydrophilicity, the paracellular pathway is probably preferred. This scenario is consistent with ~50% reduction in the Papp's of these FD's when the experimental temperature was lowered from 37°C to 4°C (Fig. 3). Theoretically, if passive diffusion is the predominant transport mechanism, the solute Papp at 4°C is expected to decrease by about 60% from that at 37°C because of a decrease in solute diffusivity (along with solvent viscosity increase). The deviation of FD70 and FD150 from the apparent inverse relationship (Fig. 4), coupled with the greater sensitivity (>80% reduction) to the same temperature change experienced by the larger FD's (Fig. 3), suggest the involvement of an alternative, perhaps endocytotic, pathway for transport of dextrans ≥70kDa. The lack of strong directionality in the Papp of FD70 and FD150 implicates a role for fluid-phase rather than adsorptive endocytosis. Such a pattern of behavior (e.g., strong temperature dependency and no direction dependency) was also observed for the same solutes in rat alveolar epithelial cell monolayers (18) as well as for horseradish peroxidase, a nonspecific fluid-phase endocytosis marker, in the alveolar epithelial barrier (23) and in the rabbit jejunum (24).

In comparison with literature reports (7,8), the Papp's obtained in the present study are one to two orders of magnitude smaller. For instance, in the study by Sasaki *et al.* (8), the Papp was 2.8×10^{-6} cm/s for FD4 and 1.6×10^{-6} cm/s for FD10, as compared with 3.5×10^{-8} cm/s and 1.9×10^{-8} cm/s, respectively, obtained in the present study. A direct comparison with the findings in the study by Hämäläinen *et al.* (7) is not as straightforward, since these authors used polyethylene glycols over the molecular weight range of 238–942 daltons. Nevertheless, the Papp was 6×10^{-6} cm/s for PEG942 (7), as compared with an estimated value of 1.2×10^{-7} cm/s for FD of comparable molecular weight. The higher values previously reported are probably the manifestation of the well known "edge effects" (17) associated with a smaller surface area (0.28 cm^2) in the Hämäläinen *et al.*'s study (7). Whereas equivalent pore analysis of the log Papp vs. solute radius relationship, as shown in Fig. 4, of our studies revealed a single population of pores 5.5 nm in radius at a density of 1.9×10^8 pores per cm^2, the same analysis applied to the data of Hämäläinen *et al.* (7) revealed pores 3.2 nm in radius at a density $2.8 \times 10^{11}/cm^2$. Conceptually, therefore, the 10^3 times higher pore density is possibly responsible, at least in part, for the approximately 50 times larger Papp for the solutes evaluated by Hämäläinen *et al.* (7) relative to those found in the present study. The pore density of $2.0 \times 10^7/cm^2$ reported by Hämäläinen *et al.* (7) is probably an underestimate of the actual pore density, and the correctness of the calculation based on the so-called effusion approach (7) and their assumption of the probability of mole-

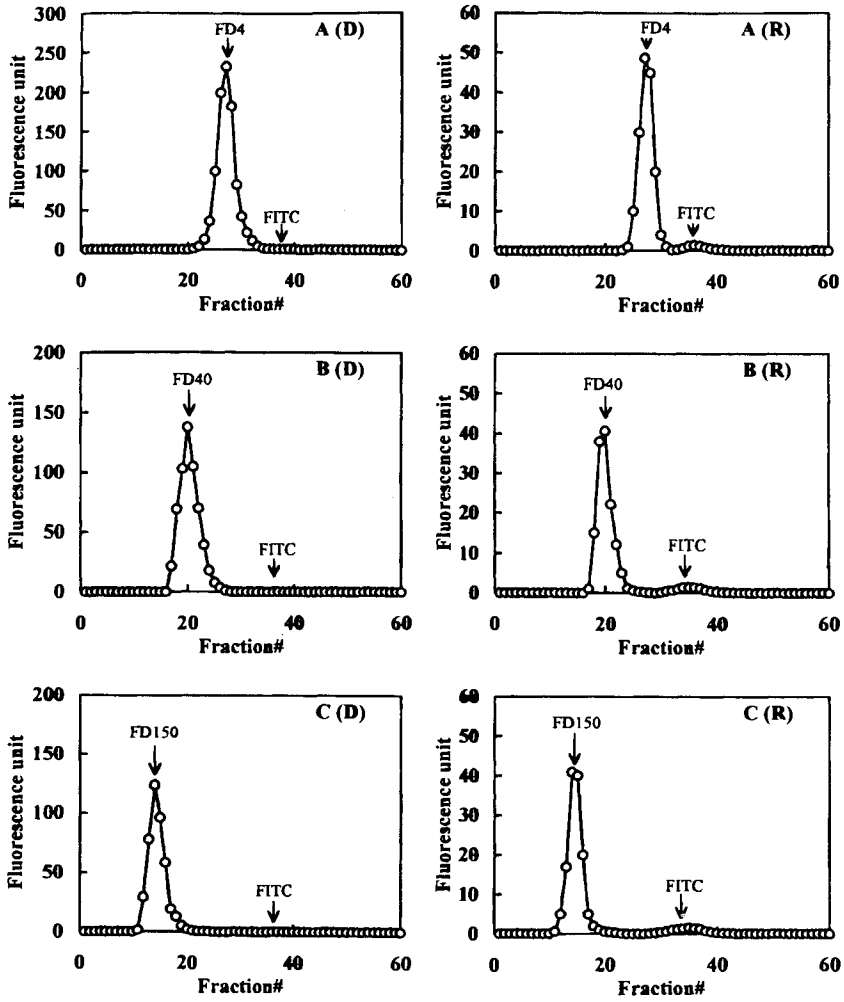

Fig. 2. Fluorescence chromatograms for FITC-labels in the mucosal donor and serosal receiver fluid collected at the end of experiments with FD4 (panel A), FD40 (panel B), and FD150 (panel C) at a donor fluid concentration of 5 mg/ml [(D): donor fluid, (R): receiver fluid]. Each fraction represents one minute and the volume is 0.4 ml.

cules to find a pore being the limiting factor (but not the hindered permeation in the pore) need to be reassessed.

Applying the effusion approach to the transport data in the present study, a porosity of 2.66×10^{-7}, a pore size of 2.8 nm, and a pore density of $1.12 \times 10^4/cm^2$ were obtained. These contrast with the corresponding values of 1.71×10^{-6}, 3.0 (bulbar conjunctiva) to 4.9 nm (palpebral conjunctiva), and $2.02 \times 10^7/cm^2$ of Hämäläinen *et al.*'s recent report (7). Moreover, when Hämäläinen *et al.*'s data (7) were subjected to a correlation analysis between $P^{PEG}_{observed}/P^{942\ dalton\ PEG}_{observed}$ and $D^{PEG}/D^{942\ dalton\ PEG}$, a linear relation was revealed. This suggests that Hämäläinen *et al.*'s data (7) contain a strong dependence on free but not restricted diffusion-limited pathways (25). When a similar analysis was applied to our present data, a hyperbolic relation was observed, suggesting the lack of systematic leaks via free diffusion-limited pathways (i.e., edge-damaged routes).

From the drug delivery point of view, it would be desirable to increase the permeability of the conjunctiva to polar solutes that opt for the paracellular pathway for transport. 8-BrcAMP (at 1 mM), which has been shown to enhance the paracellular permeability of goldfish intestinal epithelium (14), significantly increased the conjunctival permeability to mannitol, FD4 and FD40 by 23%, 31%, and 29%, respectively, with a concomitant 20–29% reduction in TEER (Table 1). On the other hand, FD150 transport was not significantly altered by 8-BrcAMP (Table 1), suggesting that fluid phase endocytosis was probably not affected by the agent. The Papp increases observed through mannitol to FD40 by cAMP were less than the 190% increase in the Papp reported for another polar drug, cidofovir (m.w. 278) (26), when the TEER was reduced by 40% upon lowering the solution tonicity from 300 to 80 mOsm/kg. The 8-BrcAMP-induced increases in Papp for solutes up to 40kDa were also much less than the 460% increase in the Papp reported for FD10 in conjunctivas exposed to 0.5% EDTA (8). More aggressive measures than 8-BrcAMP treatment, that perhaps may damage the tissue barrier, are therefore necessary to bring about marked increases in conjunctival permeability to solutes within the size range spanned by mannitol and FD40. It is estimated that the pore density would be $2.4 \times 10^8/cm^2$ in the presence of 1 mM 8-BrcAMP, a 26% increase from baseline. However, we do not know the structural correlates for this apparent density increase in "equivalent" pores in the tissue.

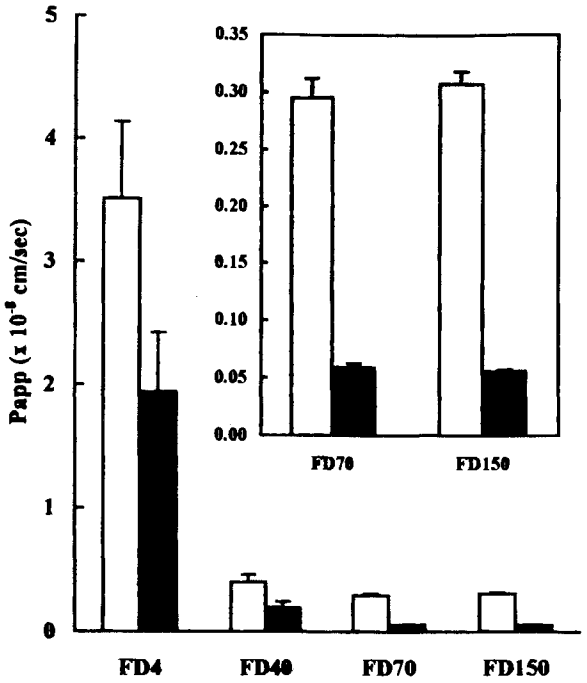

Fig. 3. Effect of temperature on Papp in the mucosal-to-serosal direction for FD4 to FD150. Inset shows an enlargement for FD70 and FD150 data. Each data point represents mean ± s.e.m. (n = 3–4). (□: 37°C, ■: 4°C).

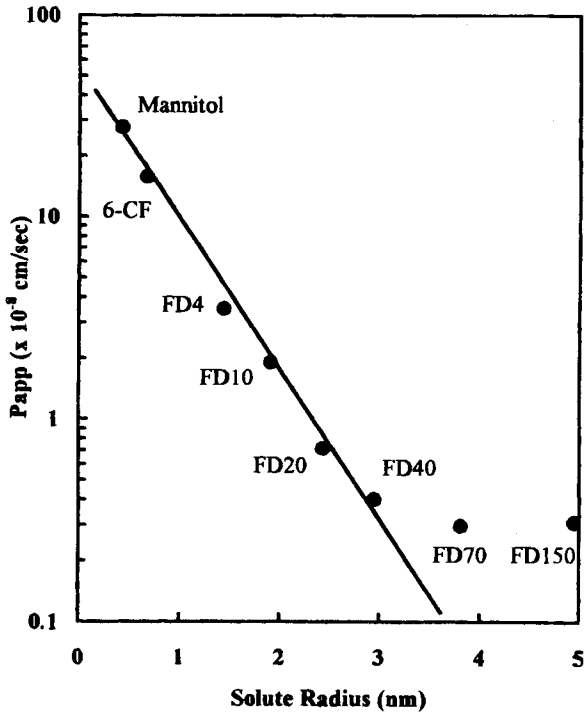

Fig. 4. Log Papp for polar solutes observed for pigmented rabbit conjunctiva at 37°C versus solute radius. The solid line shows the theoretical relationship between Papp and solute radii according to Equation 2. The experimental data for FD70 and FD150 were excluded from the analysis (see text for details).

In summary, the pigmented rabbit conjunctiva is permeable to polar solutes over the size range of 182–167,000 daltons. There appears to be a single population of pores, 5.5 nm in radius at a density of 1.9×10^8 pores/cm^2, through which mannitol through FD40 may permeate. Conceivably, the conjunctiva may also be modeled to be functionally equivalent to contain an additional population of smaller pores, through which mannitol may opt for transport. FD70 and FD150, on the other hand, may be excluded from restricted diffusion pathways and appear to rely on fluid-phase endocytosis for transport. 8-BrcAMP is marginally effective in enhancing the permeability of mannitol through FD40 and not at all effective for larger dextrans (e.g., FD150).

ACKNOWLEDGMENTS

This study was supported in part by NIH Grants EY10421 (VHLL) and HL38658 (KJK).

REFERENCES

1. M. G. Doane, A. D. Jensen, and C. H. Dohlman. *Am. J. Ophthalmol.* **85**:383–386 (1978).
2. I. Ahmed and T. F. Patton. *Int. J. Pharm.* **38**:9–21 (1987).
3. A. J. W. Huang, S. C. G. Tseng, and K. R. Kenyon. *Invest. Ophthalmol. Vis. Sci.* **30**:684–689 (1989).
4. I. Ahmed and T. F. Patton. *Invest. Ophthalmol. Vis. Sci.* **26**:584–587 (1985).
5. W. Wang, H. Sasaki, D. S. Chein, and V. H. L. Lee. *Curr. Eye Res.* **10**:571–579 (1991).
6. E. Hayakawa, D. S. Chein, K. Inagaki, A. Yamamoto, W. Wang, and V. H. L. Lee. *Pharm. Res.* **9**:769–775 (1992).
7. K. M. Hämäläinen, K. Kananen, S. Auriola, K. Kontturi, and A. Urtti. *Invest. Ophthalmol. Vis. Sci.* **38**:627–634 (1997).
8. H. Sasaki, K. Yamamura, C. Tei, K. Nishida, and J. Nakamura. *J. Drug Targeting.* **3**:129–135 (1995).
9. U. B. Kompella, K. J. Kim, M. H. I. Shiue, and V. H. L. Lee. *J. Ocular Pharmacol. Therap.* **12**:281–287 (1996).
10. E. Krasny, Jr., J. Madara, D. DiBona, and R. A. Frizzell. *Fed. Proc.* **42**:1100 (1983).
11. R. Bakker and J. A. Groot. *Am. J. Physiol.* **246**:G213–G217 (1984).
12. M. C. Rao, N. T. Nash, and M. Field. *Am. J. Physiol.* **246**:C167–C171 (1984).
13. H. R. Jacobson. *Am. J. Physiol.* **236**:F71–F79 (1979).
14. R. Bakker, K. Dekker, H. R. De-Jonge, and J. A. Groot. *Am. J. Physiol.* **264**:R362–R368 (1993).
15. B. L. Varlet, R. Ducroc, F. B. Dagonet, Y. Pouliquen, A. Vandewalle, and M. Hirsch. *Invest. Ophthalmol. Vis. Sci.* **36**:2503–2513 (1995).
16. U. B. Kompella, K. J. Kim, and V. H. L. Lee. *Curr. Eye Res.* **12**:1041–1048 (1993).
17. K. J. Kim, and E. D. Crandall. *J. Appl. Physiol.* **54**:140–146 (1983).
18. Y. Matsukawa, V. H. L. Lee, E. D. Crandall, and K. J. Kim. *J. Pharm. Sci.* **86**:305–309 (1997).
19. K. Yamaoka, Y. Tanigawara, T. Nakagawa, and T. Uno. *J. Pharmacobiodyn.* **4**:879–885 (1981).
20. B. D. Srinivasan, F. A. Jakobiec, and T. Iwamoto. Conjunctiva. In F. A. Jakobiec (ed), *Ocular Anatomy, Embryology, and Teratology*, Harper & Row, Philadelphia, 1982, pp. 733–760.
21. K. Hosoya, U. B. Kompella, K. J. Kim, and V. H. L. Lee. *Curr. Eye Res.* **15**:447–451 (1996).
22. L. Gonzalez-Mariscal, B. Chavez de Ramirez, and M. Cerejido. *J. Membr. Biol.* **79**:175–184 (1984).
23. Y. Matsukawa, H. Yamahara, V. H. L. Lee, E. D. Crandall, and K. J. Kim. *Pharm. Res.* **13**:1331–1335 (1996).
24. M. Heyman, R. Ducroc, J.-F. Desjeux, and J. L. Morgat. *Am. J. Physiol.* **242**:G558–G564 (1982).
25. C. H. van Os, M. D. de Jong, and J. F. G. Slegers. *J. Membr. Biol.* **15**:363–382 (1974).
26. K. Hosoya and V. H. L. Lee. *Curr. Eye Res.* **16**:693–697 (1997).